Downlink MIMO Diversity with Maximal-Ratio Combining in Heterogeneous Cellular Networks

Ralph Tanbourgi and Friedrich K. Jondral

***Abstract*—We present a stochastic model for analyzing the performance of multiple-input multiple-output (MIMO) diversity in a downlink heterogeneous cellular network. Multi-antenna receivers are assumed to perform maximal-ratio combining (MRC). We consider interference-blind (IB) MRC and interference-aware (IA) MRC, where the latter takes the interference power at each antenna into account. Using tools from stochastic geometry, we derive the coverage probability for both types of MRC as a function of various tier-specific system parameters, including the number of base station transmit antennas in each tier. The model is then used to compare the performance of IB-MRC and IA-MRC. One important insight is that IA-MRC becomes less favorable than IB-MRC in a transmit-diversity system due to a larger interference correlation across receive antennas.**

***Index Terms*—MIMO, space-time coding, maximal-ratio combining, coverage probability, Poisson point process.**

I. Introduction

One way to face the steadily increasing rate demands in downlink cellular systems is adding more antennas to both base stations (BSs) and user devices, and using multiple-input multiple-output (MIMO) techniques [1]. MIMO schemes can be roughly divided into open-loop and closed-loop based. Many works on MIMO cellular networks have been focusing on closed-loop schemes, such as spatial-multiplexing or multi-user MIMO, showing that tremendous gains can be harvested when channel state information is available at the transmitter (CSI-T). However, CSI may not always be available/reliable in practice and one has to resort to open-loop MIMO schemes in this case. For instance, in 3GPP LTE, transmission mode 2 is used for transmit-diversity with space-frequency block codes over two or four antennas [2]. Besides, mobile devices typically have space/complexity limitations per design, thereby often not allowing more than two antennas and requiring only simple linear combining schemes. One such combining scheme is maximal-ratio combining (MRC) [3], which offers an acceptable trade-off between performance and complexity, and is therefore ubiquitously found in multi-antenna receivers.

There exist two types of MRC, namely *interference-blind* (IB) and *interference-aware* (IA) MRC. The former —and mostly considered— ignores the different interference powers at the receive (Rx) antennas at the combining stage, while the latter takes them into account though still treating interference as white noise. Measuring the per-antenna interference power can be done within the channel estimation phase. Both types of MRC are well-understood for networks with fixed geometry, see for instance [3], [4], and recently also for ad hoc networks [5]–[8]. IA-MRC was studied in [9] for single-tier cellular networks with one transmit (Tx) antenna.

Unfortunately, analyzing MIMO diversity in the context of heterogeneous cellular networks (HetNets) is difficult due to the deployment of multiple tiers, limited site-planning, etc. [10]. In particular, spatial interference correlation across Rx antennas, which is known to have a detrimental effect on diversity combining schemes, is difficult to characterize. In order to properly assess the performance of MRC in HetNets under different MIMO settings, a realistic model and meaningful analysis covering the above aspects is hence necessary. This is the main motivation of this work. In this paper, we study the coverage performance of a downlink MIMO heterogeneous cellular system, where mobile receivers employ IB-MRC or IA-MRC. Our main contributions are summarized below.

Analytical Model: We develop a tractable stochastic model for downlink MIMO diversity with orthogonal space-time block codes (OSTBCs) and IB-MRC/IA-MRC in Section III. The model captures relevant tier-specific parameters, such as BS density and Tx power, path loss exponent, and number of Tx antennas. We derive the coverage probability for both types of MRC, while for IA-MRC we focus on two Rx-antenna case.

Design Insights: In a typical three-tier scenario with multiple Tx antennas at the BSs and IB-MRC, the gain of doubling the number of Rx antennas is roughly 2.5 dB at practical target coverage probabilities around 80%. For IA-MRC, the corresponding gain is around 3.6 dB. Besides, adding more Tx antennas has only a minor impact on the performance of IA-MRC; the coverage probability gain when adding a second Tx antenna is less than 5%. Relative to IB-MRC, IA-MRC improves the coverage probability by roughly 1.5% for the single Tx-antenna case, while this relative gain decreases to no more than 1% when Alamouti space-time coding is performed over two Tx antennas. This loss in relative performance is due to the fading-averaging effect of transmit diversity, which increases with the number of Tx antennas. Although interference power estimation required by IA-MRC can usually be realized with acceptable effort, this result suggests that IA-MRC is less favorable than IB-MRC in a MIMO HetNet with Tx diversity.

II. System Model

A. Network Geometry and User Association

We consider a K-tier HetNet in the downlink with BSs irregularly scattered in the plane, see Fig. 1. We model the irregular BS locations in tier k by an independent stationary planar Poisson point Process (PPP) Φ_k with density λ_k. We

The authors are with the Karlsruhe Institute of Technology, Communications Engineering Lab, Germany. Email: ralph.tanbourgi@kti.edu, friedrich.jondral@kit.edu.

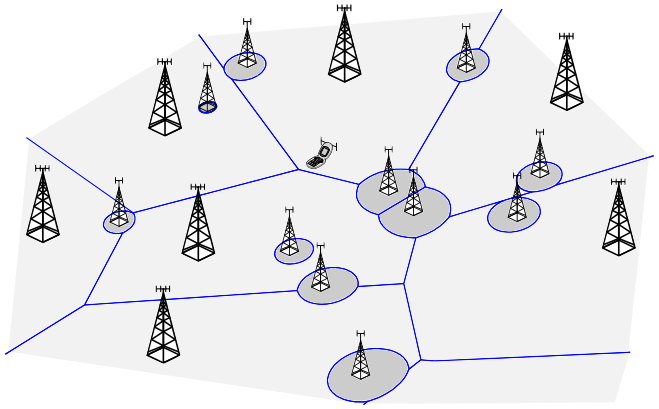

Fig. 1. Example: Downlink HetNet with $K = 2$. Tier-1 (macro) BSs have 4 antennas Tier-2 (small-cell) BSs have 2 antennas. Typical user has 2 antennas.

denote by $\Phi \triangleq \cup_{k=1}^{K} \Phi_k$ the entire set of BSs. The spatial Poisson model is widely-accepted for analyzing (multi-tier) cellular networks, see for instance [11], [12]. All BSs in tier k transmit an OSTBC using M_k Tx antennas. Similarly, we assume that mobile receivers (users) are equipped with N Rx antennas. The users are independently distributed on the plane according to some stationary point process. By Slivnyak's Theorem [13] and due to the stationarity of Φ, we can focus the analysis on a *typical* user located at the origin $o \in \mathbb{R}^2$. At the typical user, the long-term power received from a tier k BS located at $\mathsf{x}_i \in \Phi_k$ is $P_k \|\mathsf{x}_i\|^{-\alpha_k}$, where P_k is the BS Tx power in tier k, which is equally divided across all M_k Tx antennas, and $\|\cdot\|^{-\alpha_k}$ is the distance-dependent path loss with path loss exponent $\alpha_k > 2$. We assume independent and identically distributed (i.i.d) frequency-flat Rayleigh fading.

Users are assumed to associate with the BS providing the strongest average received power. For the typical user, the serving BS is hence the one maximizing $P_k \|\mathsf{x}_i\|^{-\alpha_k}$. Without loss of generality, we label the location of this BS by x_o and denote by $\mathsf{y} \triangleq \|\mathsf{x}_o\|$ its distance to the typical user. For convenience, we define $\Phi^o \triangleq \Phi \setminus \{\mathsf{x}_o\}$ (similarly, $\Phi_k^o \triangleq \Phi_k \setminus \{\mathsf{x}_o\}$), i.e., the set of interfering BSs. From the association rule discussed above it follows that, given $\mathsf{y} = y$ and that the serving BS is from tier ℓ, Φ_k^o is a homogeneous PPP on $\mathbb{R}^2 \setminus b(0, d_k)$, where $d_k = \hat{P}_k^{1/\alpha_k} y^{1/\hat{\alpha}_k}$ with $\hat{P}_k \triangleq P_k/P_\ell$ and $\hat{\alpha}_k \triangleq \alpha_k/\alpha_\ell$.

It will be useful in the later analysis to know the probability that a user associates with a certain tier k as well as the conditional probability density function (PDF) of the distance to the serving BS, which are given in the next lemma.

Lemma 1 (Association Probability and Distance PDF [14])**.** *A user associates with the ℓ-th tier with probability*

$$A_\ell = 2\pi\lambda_\ell \int_0^\infty y \exp\left(-\pi \sum_{k=1}^{K} \lambda_k \hat{P}_k^{2/\alpha_k} y^{2/\hat{\alpha}_k}\right) \mathrm{d}y. \quad (1)$$

The PDF of the distance $\mathsf{y} \triangleq \|\mathsf{x}_o\|$ to the serving BS, given that it belongs to tier ℓ, is

$$f_{\mathsf{y}}(y) = \frac{2\pi\lambda_\ell y}{A_\ell} \exp\left(-\pi \sum_{k=1}^{K} \lambda_k \hat{P}_k^{2/\alpha_k} y^{2/\hat{\alpha}_k}\right), \quad y \geq 0. \quad (2)$$

B. OSTBC MIMO Signal Model

All BSs of the k-th tier use an (M_k, T_k, r_k)-OSTBC, where $T_k \geq 1$ is the codeword length and $r_k \in (0, 1]$ is the code rate; T_k can be seen as the number of slots (number of channel uses) for conveying $S_k = T_k r_k$ symbols using M_k Tx antennas. For analytical tractability, we shall consider only *power-balanced* (M_k, T_k, r_k)-OSTBCs, i.e., having the property that exactly S_k symbols are transmitted, or equivalently that $S_k \leq M_k$ Tx antennas are active, in every slot of the codeword. This will allow us to assign a constant power load of P_k/S_k to every symbol-antenna pair. Practical examples of balanced OSTBCs are $(1, 1, 1)$ (single-antenna), $(2, 2, 1)$ (Alamouti), $(4, 4, 1/2)$, and $(4, 4, 3/4)$, see [15], [16] for instance. We use the notation $\mathbf{v}_{i,\tau} \in \{0, 1\}^{M_k}$ to indicate which Tx antennas of BS i are active in slot τ, i.e., the m-th entry of $\mathbf{v}_{i,\tau}$ is equal to one if Tx antenna m is active and zero otherwise.

Assume for the moment that the typical user associates with the ℓ-th tier. It will then be served by an (M_ℓ, T_ℓ, r_ℓ)-OSTBC. The interference-plus-noise corrupted received signal at the typical user in slot $\tau \in \{1, \ldots, T_\ell\}$ can then be expressed by

$$\mathbf{y}_\tau = \mathbf{H}_o\, \mathbf{c}_{o,\tau} + \sum_{k=1}^{K} \sum_{\mathsf{x}_i \in \Phi_k^o} \mathbf{H}_i\, \mathbf{c}_{i,\tau} + \mathbf{n}_\tau, \quad (3)$$

where

- $\mathbf{H}_i \in \mathbb{C}^{N \times M_k}$ is the channel fading matrix between the i-th BS of the k-th tier and the typical user. The elements of $\mathbf{H}_i$, denoted by $\mathsf{h}_{i,nm}$, are $\mathcal{CN}(0, 1)$ distributed and remain constant over one codeword period. We assume that $\mathbb{E}[\mathsf{h}_{i,nm} \mathsf{h}_{j,uv}^*] = 0$ unless $i = j$, $n = u$, and $m = v$.
- $\mathbf{c}_{i,\tau} \in \mathbb{C}^{M_k}$ are the space-time coded symbols of the i-th BS sent over the M_k Tx antennas in slot τ. We assume $\mathbb{E}\left[\mathbf{c}_{i,\tau} \mathbf{c}_{j,\tau}^H\right] = 0$ for all $i \neq j$ and $\mathbb{E}[\mathbf{c}_{i,\tau}] = 0$ element-wise. Furthermore, it is reasonable to assume $\mathbb{E}[\mathbf{c}_{i,\tau} \mathbf{c}_{i,\tau}^H] = \frac{P_k}{S_k \|\mathsf{x}_i\|^{\alpha_k}} \mathrm{diag}(\mathbf{v}_{i,\tau})$, where $\mathrm{diag}(\mathbf{v}_{i,\tau})$ is a diagonal matrix with entries $\mathbf{v}_{i,\tau}$. The latter follows from the balanced-power property of the considered OSTBCs.
- $\mathbf{n}_\tau \in \mathbb{C}^N$ is a vector describing the Rx noise with independent $\mathcal{CN}(0, \sigma^2)$ distributed entries.

Upon receiving all T_ℓ code symbols of the desired codeword to be decoded, the typical user stacks the vectors $\mathbf{y}_1, \ldots, \mathbf{y}_{T_\ell}$ to form the new vector

$$\bar{\mathbf{y}} = \begin{bmatrix} \mathbf{H}_o\, \mathbf{c}_{o,1} \\ \vdots \\ \mathbf{H}_o\, \mathbf{c}_{o,T_\ell} \end{bmatrix} + \sum_{k=1}^{K} \sum_{\mathsf{x}_i \in \Phi_k^o} \underbrace{\begin{bmatrix} \mathbf{H}_i\, \mathbf{c}_{i,1} \\ \vdots \\ \mathbf{H}_i\, \mathbf{c}_{i,T_\ell} \end{bmatrix}}_{\bar{\mathbf{i}}_i} + \begin{bmatrix} \mathbf{n}_1 \\ \vdots \\ \mathbf{n}_{T_\ell} \end{bmatrix}, \quad (4)$$

where $\bar{\mathbf{i}}_i \in \mathbb{C}^{NT_\ell}$ is the interference signal from the i-th BS received over the entire codeword period. With CSI-R, $\bar{\mathbf{y}}$ is linearly processed using MRC to form the final decision variable. Two types of MRC are considered, which differ in the amount of CSI needed. Moe specifically, IB-MRC requires knowledge of $\mathbf{H}_o$, while IA-MRC additionally needs to know the interference-plus-noise power at each Rx antenna. The following lemma will be useful in the later analysis.

Lemma 2 (Gaussian Matrices)**.** *Let the matrix $\mathbf{X}(u) \in \mathbb{C}^{v\times w}$ have $u \leq vw$ $\mathcal{CN}(0,1)$-distributed entries and $vw-u$ zeros. Then $\|\mathbf{X}(u)\|_F^2$ is Erlang distributed with CDF*

$$\mathbb{P}(\|\mathbf{X}(u)\|_F^2 \leq \theta) = 1 - e^{-\theta}\sum_{j=0}^{u-1}\frac{\theta^j}{j!}. \quad (5)$$

Let $\mathbf{h}_{i,n} = [\mathsf{h}_{i,n1}, \ldots, \mathsf{h}_{i,nM_k}]$ be the n-th row of $\mathbf{H}_i$. Then, the interference power in slot τ (we shall drop this index in the following) measured at the n-th Rx antenna, averaged over the interfering code symbols $\mathbf{c}_i$, is

$$\begin{aligned}\mathsf{I}_n &= \mathbb{E}_{\mathbf{c}_i}\left[\left(\sum_{k=1}^{K}\sum_{\mathsf{x}_i\in\Phi_k^o}\mathbf{h}_{i,n}\mathbf{c}_i\right)\left(\sum_{k=1}^{K}\sum_{\mathsf{x}_i\in\Phi_k^o}\mathbf{h}_{i,n}\mathbf{c}_i\right)^H\right]\\ &\overset{(a)}{=}\sum_{k=1}^{K}\sum_{\mathsf{x}_i\in\Phi_k^o}\mathbf{h}_{i,n}\mathbb{E}\left[\mathbf{c}_i\mathbf{c}_i^H\right]\mathbf{h}_{i,n}^H\\ &\overset{(b)}{=}\sum_{k=1}^{K}\sum_{\mathsf{x}_i\in\Phi_k^o}\frac{P_k}{S_k\|\mathsf{x}_i\|^{\alpha_k}}\mathbf{h}_{i,n}\mathrm{diag}(\mathbf{v}_i)\mathbf{h}_{i,n}^H\\ &=\sum_{k=1}^{K}\sum_{\mathsf{x}_i\in\Phi_k^o}\frac{P_k}{S_k\|\mathsf{x}_i\|^{\alpha_k}}\|\mathbf{h}_{i,n}(S_k)\|_F^2, \quad (6)\end{aligned}$$

where (a) follows from the independence between the $\mathbf{c}_i$ across BSs and (b) follows from the correlation properties of the $\mathbf{c}_i$.

Remark 1 (Feasibility of Interference Power Estimation)**.** *When the set of active antennas of interfering BSs changes in every slot τ, I_n varies unpredictably from slot to slot. This is the case when $S_k < M_k$. Unfortunately, such rapid variations over τ are imperceptible to CSI estimation since the latter is usually designed to track channel-fading variations, which happen on a larger time scale. However, when full-rate OSTBCs are used ($r_k = 1$ for all k), I_n is identical across τ. In that case, the receiver can obtain knowledge of I_n with acceptable complexity, e.g., by estimating it once within one frame using techniques from [17], [18].*

III. Coverage Probability Analysis

We now study the downlink performance at the typical user for both IB-MRC and IA-MRC. As explained in Remark 1, IA-MRC is practical only for full-rate OSTBCs ($r_k = 1$ for all k). A common way for studying the performance of diversity-combining techniques is to analyze the post-combiner signal-to-interference-plus-noise ratio (SINR). The specific form of the SINR depends on the considered scheme and will be derived in Sections III-A and III-B.

Definition 1 (Coverage Probability $\mathtt{P_c}$)**.** *The coverage probability at the typical user is defined as*

$$\mathtt{P_c} \triangleq \mathbb{P}\left(\mathtt{SINR} \geq T\right) \quad (7)$$

for a coding and modulation specific threshold $T > 0$.

The $\mathtt{P_c}$ can be interpreted as the SINR distribution at the typical user, or alternatively as the average fraction of users in the network covered by an SINR no less than T [14].

A. MIMO Diversity with interference-blind MRC

An extremely useful property of OSTBCs is that the MIMO input-output relation, i.e., (4), can be reduced to parallel SISO channels [19]. At the typical user, having knowledge of $\mathbf{H}_o$, this is achieved by performing the linear combination $\sum_{n=1}^{N}\sum_{m=1}^{M_\ell}\mathsf{h}_{o,nm}^*\mathbf{A}_{nm}^H\bar{\mathbf{y}} + \mathsf{h}_{o,nm}\mathbf{B}_{nm}^T\bar{\mathbf{y}}^*$, where $\mathbf{A}_{nm}$ and $\mathbf{B}_{nm}$ are the dispersion matrices describing the OSTBC employed in the serving tier, see [20], [21] for further details. The resulting *equivalent channel model* allows treating the detection of each of the S_ℓ information symbols encoded in the current codeword separately. The corresponding SINR at the symbol decoder can then be expressed as

$$\mathtt{SINR}_\ell(y) = \frac{\frac{P_\ell}{S_\ell y^{\alpha_\ell}}\|\mathbf{H}_o\|_F^2}{\sum_{k=1}^{K}\sum_{\mathsf{x}_i\in\Phi_k^o}\mathsf{I}_{i,\text{eqv}} + \sigma^2}, \quad (8)$$

where $\mathsf{I}_{i,\text{eqv}}$ is the interference power from the i-th BS in the equivalent channel model. $\mathsf{I}_{i,\text{eqv}}$ is statistically the same for all S_ℓ symbols. Thus, focusing on an arbitrary symbol, i.e., considering a single arbitrary column of $\mathbf{A}_{nm}$, $\mathbf{B}_{nm}$, say $\mathbf{a}_{nm}$, $\mathbf{b}_{nm}$, the interference power $\mathsf{I}_{i,\text{eqv}}$ is

$$\mathsf{I}_{i,\text{eqv}} = \mathrm{Var}_{\mathbf{c}_i}\left[\sum_{n=1}^{N}\sum_{m=1}^{M_\ell}\frac{\mathsf{h}_{o,nm}^*}{\|\mathbf{H}_o\|_F}\mathbf{a}_{nm}^H\bar{\mathbf{i}}_i + \frac{\mathsf{h}_{o,nm}}{\|\mathbf{H}_o\|_F}\mathbf{b}_{nm}^T\bar{\mathbf{i}}_i^*\right]. \quad (9)$$

Note that the Rx noise statistics remain unaffected by the linear combination [19], [21]. However, the distribution of $\mathsf{I}_{i,\text{eqv}}$ is more complicated, particularly due to its dependence on $\mathbf{H}_o$. This was already observed in [5] for a similar MIMO network model, where the authors also showed that ignoring this dependence and assuming $\mathsf{I}_{i,\text{eqv}}$ to be Gamma distributed yields a valid approximation. We shall thus follow the same approach and assume $\mathsf{I}_{i,\text{eqv}} \simeq \frac{P_k}{S_k\|\mathsf{x}_i\|^{\alpha_k}}\|\mathbf{H}_i(S_k)\|_F^2$ with $\mathsf{I}_{i,\text{eqv}}$ being independent from $\mathbf{H}_o$. The following two facts support this approximation:

- It can be shown that the approximation is moment matching irrespective of the realization of $\mathbf{H}_o$, i.e., $\mathbb{E}_{\mathbf{H}_i}[\mathsf{I}_{i,\text{eqv}}] = \frac{P_k}{S_k\|\mathsf{x}_i\|^{\alpha_k}}\mathbb{E}_{\mathbf{H}_i}[\|\mathbf{H}_i(S_k)\|_F^2] = \frac{P_k}{\|\mathsf{x}_i\|^{\alpha_k}}$ in (9).
- Whenever $M_k = 1$, it follows from [15] that the above approximation becomes exact. In this case $\mathsf{I}_{i,\text{eqv}}$ is also truly independent from $\mathbf{H}_o$.

Lemma 3 (Interference Laplace Transform)**.** *Consider the interference field $\mathsf{I} = \sum_{k=1}^{K}\sum_{\mathsf{x}_i\in\Phi_k^o}\frac{P_k}{S_k\|\mathsf{x}_i\|^{\alpha_k}}\|\mathbf{H}_i(S_k)\|_F^2$. Its Laplace transform is given by*

$$\mathcal{L}_{\mathsf{I}}(s) = e^{-\pi\sum_{k=1}^{K}\lambda_k d_k^2\left({}_2F_1\left(-\frac{2}{\alpha_k},S_k,1-\frac{2}{\alpha_k};-\frac{sP_k}{S_k d_k^{\alpha_k}}\right)-1\right)}. \quad (10)$$

Proof: We write

$$\begin{aligned}&\mathbb{E}\left[\exp\left(-s\sum_{k=1}^{K}\sum_{\mathsf{x}_i\in\Phi_k^o}\frac{P_k}{S_k\|\mathsf{x}_i\|^{\alpha_k}}\|\mathbf{H}_i(S_k)\|_F^2\right)\right]\\ &\overset{(a)}{=}\prod_{k=1}^{K}\mathbb{E}\left[\prod_{\mathsf{x}_i\in\Phi_k^o}\mathcal{L}_{\|\mathbf{H}_i(S_k)\|_F^2}\left(\frac{sP_k}{S_k\|\mathsf{x}_i\|^{\alpha_k}}\right)\right]\end{aligned}$$

$$\mathtt{P}_{\mathrm{c}}^{\mathrm{IB}} = 2\pi \sum_{\ell=1}^{K} \sum_{m=0}^{NM_\ell - 1} \frac{(-1)^m \lambda_\ell}{m!} \int_0^\infty y \, \frac{\mathrm{d}^m}{\mathrm{d}s^m} \left[\exp\left(-\frac{sS_\ell T}{\mathtt{SNR}_\ell(y)} - \pi \sum_{k=1}^{K} \lambda_k \hat{P}_k^{2/\alpha_k} y^{2/\hat{\alpha}_k} \, {}_2F_1\!\left(-\frac{2}{\alpha_k}, S_k, 1 - \frac{2}{\alpha_k}; -\frac{sT}{\hat{S}_k} \right) \right) \right]_{s=1} \mathrm{d}y \quad (12)$$

$$\mathtt{P}_{\mathrm{c}}^{\mathrm{IA}} = 2\pi \sum_{\ell=1}^{K} \sum_{m=0}^{M_\ell - 1} \frac{(-1)^{m+M_\ell} \lambda_\ell}{m! \, \Gamma(M_\ell)} \int_0^\infty \int_0^\infty y \, z^{-1} \frac{\mathrm{d}^m \, \mathrm{d}^{M_\ell}}{\mathrm{d}s^m \, \mathrm{d}t^{M_\ell}} \left[\exp\left(-\frac{M_\ell}{\mathtt{SNR}_\ell(y)} \left(s\,(T-z)^+ + tz \right) \right) \right.$$
$$\left. \times \exp\left(-\pi \sum_{k=1}^{K} \lambda_k \hat{P}_k^{2/\alpha_k} y^{2/\hat{\alpha}_k} \left[1 + \Psi\left(\frac{s\,(T-z)^+}{\hat{M}_k}, \frac{tz}{\hat{M}_k}, M_k, \alpha_k \right) \right] \right) \right]_{\substack{s=1 \\ t=1}} \mathrm{d}y \, \mathrm{d}z, \quad 1 \le M_k \le 2, N = 2 \quad (20)$$

$$\overset{\text{(b)}}{=} \exp\left\{ -\pi \sum_{k=1}^{K} \lambda_k \int_{d_k}^{\infty} 2r \left(1 - \left(1 + \tfrac{sP_k}{S_k r^{\alpha_k}} \right)^{-S_k} \right) \mathrm{d}r \right\}, \quad (11)$$

where (a) follows from the independence of the Φ_k^o across k and of the independence of the $\|\mathbf{H}_i(S_k)\|_F^2$ across i, and (b) follows from the probability generating functional (PGFL) for PPPs, see [13]. Solving the integral yields the result ∎

We now have the tools required to characterize the coverage probability for IB-MRC. This task is addressed in the following theorem.

Theorem 1 ($\mathtt{P}_{\mathrm{c}}$ for Interference-Blind MRC)**.** *The coverage probability $\mathtt{P}_{\mathrm{c}}^{\mathrm{IB}}$ for IB-MRC in the described setting is given by* (12) *at the top of the page, where $\mathtt{SNR}_\ell(y) \triangleq P_\ell \, y^{-\alpha_\ell}/\sigma^2$ and $\hat{S}_k \triangleq S_k/S_\ell$.*

Proof: See Appendix A. ∎

The differentiation $\mathrm{d}^m/\mathrm{d}s^m$ in (12) can be calculated using Faà di Bruno's formula for higher-order derivatives of composite functions [22]. While the outer function is simple due to the exp-term, the inner function, more specifically the ${}_2F_1\!\left(-2/\alpha_k, S_k, 1-2/\alpha_k; -sT/\hat{S}_k\right)$ expression, is more involved. With [22], its derivative is obtained as

$$\frac{\mathrm{d}^m}{\mathrm{d}s^m} \left[{}_2F_1\!\left(-\frac{2}{\alpha_k}, S_k, 1 - \frac{2}{\alpha_k}; -\frac{sT}{\hat{S}_k} \right) \right]_{s=1}$$
$$= \left(-\frac{T}{\hat{S}_k} \right)^m \frac{-2/\alpha_k \, \Gamma(S_k + m)}{(m - 2/\alpha_k) \, \Gamma(S_k)}$$
$$\times {}_2F_1\!\left(-\frac{2}{\alpha_k} + m, S_k + m, 1 - \frac{2}{\alpha_k} + m; -\frac{T}{\hat{S}_k} \right). \quad (13)$$

In dense deployments the performance is typically limited by interference rather than noise [23]. In this case, one can set $\sigma^2 = 0 \Leftrightarrow 1/\mathtt{SNR}_\ell(y) = 0$. In addition, the path loss exponent does not vary significantly across tiers in practice with typical values around $\alpha_k \approx 3.7$ [24]. When also the number of Tx antennas is equal across tiers, the following corollary applies.

Corollary 1 (Special Case)**.** *In the absence of Rx noise ($\sigma^2 = 0$) and with equal path loss exponents ($\alpha_k = \alpha$) and the same number of Tx antennas ($M_k = M$, $S_k = S$), $\mathtt{P}_{\mathrm{c}}^{\mathrm{IB}}$ simplifies to*

$$\mathtt{P}_{\mathrm{c}} = \sum_{m=0}^{NM-1} \frac{(-1)^m}{m!} \frac{\mathrm{d}^m}{\mathrm{d}s^m} \left[\frac{1}{{}_2F_1\!\left(-\frac{2}{\alpha}, S, 1 - \frac{2}{\alpha}; -sT\right)} \right]_{s=1}. \quad (14)$$

The coverage probability in (14) does not depend on the BS densities λ_k and powers P_k, nor on the total number of tiers K, which is consistent with the literature, see for instance [12], [14]. Note that the first term $m = 0$ in (14) corresponds to the coverage probability for the SISO case [25].

B. MIMO Diversity with interference-aware MRC

We now assume $M_k \le 2$ for all K tiers. This ensures that the receiver can estimate the interference power with acceptable complexity once within the current block/frame, see Remark 1. In this case, we have $S_k \equiv M_k$. When $M_k \le 2$, tier k uses either Alamouti space-time coding ($M_k = 2$) or no space-time coding ($M_k = 1$). In both cases, the interference power remains constant in each codeword slot. Its value at the n-th antenna is given by (6). We assume that the receiver perfectly knows the current per-antenna interference-plus-noise power $\mathsf{I}_n + \sigma^2$ at each antenna, in addition to knowing $\mathbf{H}_o$. Interference is still treated as white noise.

In IA-MRC, the phase-corrected and channel-weighted received signals are additionally scaled by the interference-plus-noise power experienced at each antenna, thereby following the original MRC approach from [3]. The linear combination

$$\sum_{n=1}^{N} \sum_{m=1}^{M_\ell} \frac{\mathsf{h}_{o,nm}^*}{\mathsf{I}_n + \sigma^2} \mathbf{A}_{nm}^H \bar{\mathbf{y}} + \frac{\mathsf{h}_{o,nm}}{\mathsf{I}_n + \sigma^2} \mathbf{B}_{nm}^T \bar{\mathbf{y}}^*, \quad (15)$$

yields the equivalent channel model for IA-MRC. Note that now, the interference-plus-noise power is factored in. Similar to Section III-A, we focus again on an arbitrary symbol and therefore consider an arbitrary column $\mathbf{a}_{mn}$, $\mathbf{b}_{nm}$ of $\mathbf{A}_{nm}$, $\mathbf{B}_{nm}$. The SINR for IA-MRC can then be expressed as

$$\mathtt{SINR}_\ell(y) = \frac{\frac{P_\ell}{M_\ell \, y^{\alpha_\ell}} \left(\sum_{n=1}^{N} \frac{\|\mathbf{h}_{o,n}\|_F^2}{\mathsf{I}_n + \sigma^2} \right)^2}{\sum_{k=1}^{K} \sum_{\mathsf{x}_i \in \Phi_k^o} \mathsf{I}_{i,\mathrm{eqv}} + \sum_{n=1}^{N} \frac{\|\mathbf{h}_{o,n}\|_F^2 \sigma^2}{(\mathsf{I}_n + \sigma^2)^2}}, \quad (16)$$

where now $\mathsf{I}_{i,\mathrm{eqv}}$ is

$$\mathsf{I}_{i,\mathrm{eqv}} = \mathrm{Var}_{\mathbf{c}_i} \left[\sum_{n=1}^{N} \sum_{m=1}^{M_\ell} \frac{\mathsf{h}_{o,nm}^*}{\mathsf{I}_n + \sigma^2} \mathbf{a}_{nm}^H \bar{\mathbf{i}}_i + \frac{\mathsf{h}_{o,nm}}{\mathsf{I}_n + \sigma^2} \mathbf{b}_{nm}^T \bar{\mathbf{i}}_i^* \right]. \quad (17)$$

Using the orthogonality property of $\mathbf{A}_{nm}, \mathbf{B}_{nm}$, see for instance [15], we can rewrite (17) as

$$\mathsf{I}_{i,\mathrm{eqv}} = \frac{P_k}{M_k \|\mathsf{x}_i\|^{\alpha_k}} \sum_{n=1}^{N} \|\mathbf{h}_{o,n}\|_F^2 \frac{\|\mathbf{h}_{i,n}\|_F^2}{(\mathsf{I}_n + \sigma^2)^2} + \frac{\mathsf{Z}_{i,n}}{(\mathsf{I}_n + \sigma^2)^2}, \quad (18)$$

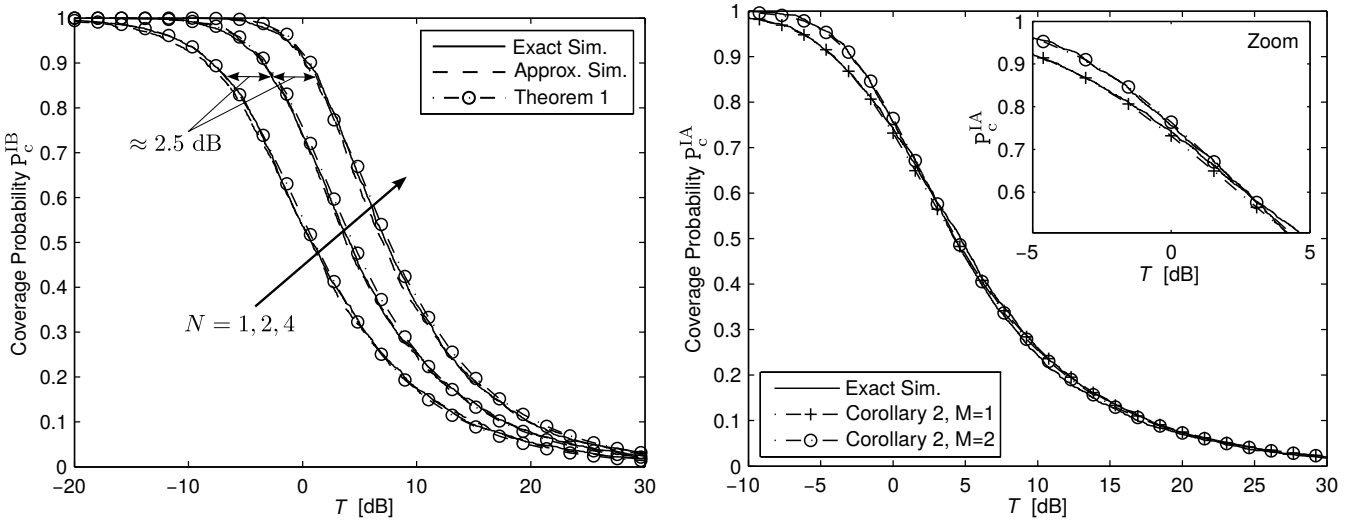

(a) Coverage probability IB-MRC (b) Coverage probability IA-MRC

Fig. 2. (a) Coverage probability $\mathtt{P}_\mathtt{c}^{\mathrm{IB}}$ for path loss exponents $\alpha_1 = 3.76$, $\alpha_2 = 3.67$, $\alpha_3 = 3.5$. Receiver noise is $\sigma^2 = -104\,\mathrm{dBm}$. (b) Coverage probability $\mathtt{P}_\mathtt{c}^{\mathrm{IA}}$ for $\alpha = 3.7$, $\sigma^2 = 0$, and $M = 1, 2$.

where $\mathsf{Z}_{i,n}$ describes the part resulting from the non-zero off-diagonal elements of the covariance matrix $\mathbb{E}_{\mathbf{c}_i}[\bar{\mathbf{i}}_i \bar{\mathbf{i}}_i^H]$. It can be shown that $\mathbb{E}_{\mathbf{H}_i}[\mathsf{Z}_{i,n}] = 0$ irrespective of $\mathbf{H}_o$. To obtain a more tractable SINR expression, we hence ignore the $\mathsf{Z}_{i,n}$ term. After some simple algebraic manipulations, the *simplified* SINR from (16) becomes

$$\mathtt{SINR}_\ell(y) = \frac{P_\ell}{M_\ell\, y^{\alpha_\ell}} \sum_{n=1}^{N} \frac{\|\mathbf{h}_{o,n}\|_F^2}{\mathsf{I}_n + \sigma^2}. \tag{19}$$

Remark 2 (SINR-Approximation)**.** *It follows by Jensen's Inequality [26] that the approximate* SINR *in* (19) *underestimates the true* SINR *in* (16)*. The resulting error, however, is barely noticeable as confirmed by simulations, see Sec. IV.*

Although the $\mathbf{h}_{i,n}$ in (19) are mutually independent, the interference terms I_n are correlated across the N Rx antennas due to the common locations of interfering BSs. More specifically, the expression in (19) is a sum of *correlated* random variables exhibiting a complicated correlation structure. This renders the characterization of the coverage probability of IA-MRC for general number of Rx antennas N challenging. In practical systems, however, the number of antennas mounted on mobile devices is limited due to space/complexity limitations, thereby often not exceeding $N = 2$ antennas. This practically relevant case is addressed in the following theorem.

Theorem 2 ($\mathtt{P}_\mathtt{c}$ for Interference-Aware MRC)**.** *The coverage probability* $\mathtt{P}_\mathtt{c}^{\mathrm{IA}}$ *for IA-MRC in the described setting with* $M_k \leq 2$ *is given by* (20) *at the top of the last page, where* $\Psi(\cdot,\cdot,\cdot,\cdot)$ *is given by* (32) *and* $\hat{M}_k \triangleq M_k/M_\ell$.

Proof: See Appendix B. ∎

Compared to $\mathtt{P}_\mathtt{c}^{\mathrm{IB}}$ in (12), $\mathtt{P}_\mathtt{c}^{\mathrm{IA}}$ is analytically more involved due to the mathematical form of (19), which translates into the convolution-type integration over z in (20). Nevertheless, the expression in (20) can be evaluated with acceptable complexity using semi-analytical tools, see for instance [8]. Moreover, $\Psi(\cdot,\cdot,\cdot,\cdot)$ can be given in terms of the Gaussian hypergeometric function, which reduces to elementary functions for suitable α_k. Besides, (20) covers the general case and the expression can be further simplified for certain scenarios as discussed next. The counterpart to Corollary 1 is given next.

Corollary 2 (Special Case)**.** *In the absence of Rx noise (*$\sigma^2 = 0$*), and with equal path loss exponents (*$\alpha_k = \alpha$*) and the same number of Tx antennas (*$M_k = M \leq 2$*),* $\mathtt{P}_\mathtt{c}^{\mathrm{IA}}$ *reduces to*

$$\mathtt{P}_\mathtt{c}^{\mathrm{IA}} = \sum_{m=0}^{M-1} \frac{(-1)^{m+M}}{m!\,\Gamma(M)} \int_0^\infty z^{-1} \times \frac{\mathrm{d}^m\,\mathrm{d}^M}{\mathrm{d}s^m\,\mathrm{d}t^M} \left[\frac{1}{1 + \Psi\left(s\,(T-z)^+, tz, M, \alpha\right)} \right]_{\substack{s=1 \\ t=1}} \mathrm{d}z. \tag{21}$$

The expression in (21) is less complicated than (20). When the SINR threshold T is not large, the $\Psi\left(s\,(T-z)^+, tz, M, \alpha\right)$ term can be further simplified as shown next.

Corollary 3 (Small-T Approximation)**.** *When* T *is small, the following approximation becomes tight*

$$1 + \Psi\left(\frac{s\,(T-z)^+}{\hat{M}_k}, \frac{tz}{\hat{M}_k}, M_k, \alpha_k\right) \simeq {}_2F_1\left(-\frac{2}{\alpha_k}, M_k, 1 - \frac{2}{\alpha_k}; -\frac{s\,(T-z)^+ + tz}{\hat{M}_k}\right). \tag{22}$$

The right-hand side of (22) may be easier to evaluate than the original expression since the Gaussian hypergeometric function is available in most numerical software programs. Moreover, its higher-order derivatives with respect to both s and t appearing in (20) can be evaluated fairly easily following the same idea as in (13).

Remark 3 (Single-Tier, Single-Tx-Antenna)**.** *Setting $K = 1$ and $M = 1$, we recover the coverage probability result from [9] for single-tier single-Tx-antenna cellular networks.*

IV. Discussion and Numerical Examples

We assume a typical three-tier HetNet setting ($K = 3$), where BSs have densities $\lambda_1 = 4\,\text{BS/km}^2$, $\lambda_2 = 16\,\text{BS/km}^2$, $\lambda_3 = 40\,\text{BS/km}^2$, and transmit powers $P_1 = 46\,\text{dBm}$, $P_2 = 30\,\text{dBm}$, $P_3 = 24\,\text{dBm}$. The dispersion matrices $\mathbf{A}_{nm}$, $\mathbf{B}_{nm}$ are obtained using [15, Sec. 2.2.3].

We first focus on IB-MRC and consider a typical scenario with $M_1 = 4$, $M_2 = 2$ (Alamouti), and $M_3 = 1$ (no space-time coding). The $(4, 4, 3/4)$-OSTBC from [16, 7.4.10] is chosen for tier one. Fig. 2a shows the coverage probability $\mathtt{P}_\mathrm{c}^{\mathrm{IB}}$ for IB-MRC and different number of Rx antennas N. It can be seen that the theoretical expressions perfectly match the simulation results. Furthermore, the simulation results for the interference Gamma approximation explained in Section III-A (Approx. Sim.) and for the exact case (Exact Sim.) are hardly distinguishable, which is consistent with [5]. As expected, increasing N improves $\mathtt{P}_\mathrm{c}^{\mathrm{IB}}$ since the typical user enjoys a larger array gain. For operation points of practical relevance, i.e. around 80% of covered users, the horizontal gap between the curves in Fig. 2a is roughly 2.5 dB. For IA-MRC, this gain is about 3.6 dB (verified through simulations).

Figure 2b shows the coverage probability $\mathtt{P}_\mathrm{c}^{\mathrm{IA}}$ for IA-MRC. Here, we consider the interference-limited case ($\sigma^2 = 0$) with equal path loss exponents ($\alpha_k = 3.7$) and the same number of Tx antennas ($M_k = M$). Again, simulation results and theoretical expressions (Corollary 2) are fairly close over the whole T-range. It can be further observed that, for IA-MRC, adding a second Tx antenna and performing Alamouti space-time coding slightly improves performance only at low T. This gain, about 4% in the practically relevant regime, is comparable to the gain due to frequency-diversity based resource allocation in HetNets with single Tx antenna [27].

Next, we compare the performance between IB-MRC and IA-MRC for the same scenario as for Fig. 2b. In Fig. 3, the relative coverage probability gain of IA-MRC over IB-MRC is shown for $M = 1$ and $M = 2$ Tx antennas. In line with the observations from [9] for single-tier single-Tx-antenna cellular networks, the gain is insignificant ($< 2\%$ in this example). In fact, IA-MRC becomes even less favorable over IB-MRC when adding more Tx antennas. This due to the fact that adding more antennas effectively averages out the fading on the interfering channels, which implies that interference power becomes even more correlated across Rx antennas. Thus, with increasing similarity of the interference level across Rx antennas, the performance of IA-MRC eventually becomes equal to that of IB-MRC.

V. Conclusion

We presented a stochastic model for analyzing downlink MIMO diversity with MRC at the receivers in heterogeneous cellular networks. We showed that transmit diversity has a considerable impact on the relative performance of IB-MRC and IA-MRC. Our results revealed that IA-MRC is only slightly better than IB-MRC when multiple Tx antennas are used. Future work may include extending the model to incorporate also other linear combing schemes in combination with transmit diversity and spatial multiplexing.

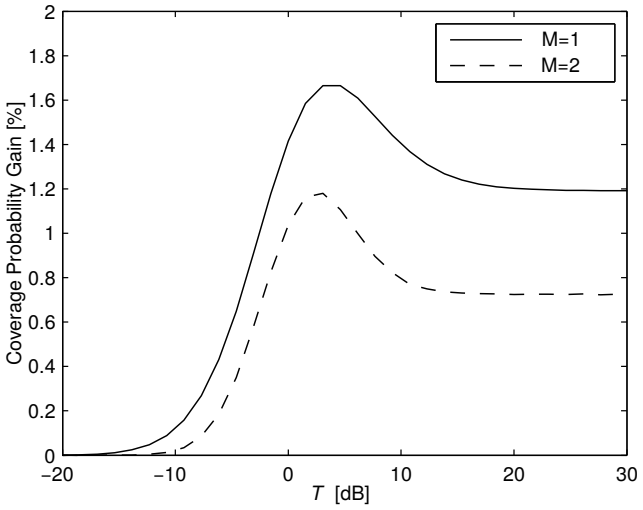

Fig. 3. Relative coverage probability gain of IA-MRC over IB-MRC for $\alpha = 3.7$, $\sigma^2 = 0$, and $M = 1, 2$.

Appendix

A. Proof of Theorem 1

Applying the law of total probability and making use of Lemma 1, we can express (7) by

$$\mathtt{P}_\mathrm{c} = \sum_{\ell=1}^{K} A_\ell \int_0^\infty f_{\mathsf{y},\ell}(y)\, \mathbb{P}\left(\mathtt{SINR}_\ell(y) \geq T\right) \mathrm{d}y, \quad (23)$$

where $\mathbb{P}\left(\mathtt{SINR}_\ell(y) \geq T\right)$ can be seen as the *conditional* $\mathtt{P}_\mathrm{c}$, given ℓ, y. With Lemma 2, the conditional $\mathtt{P}_\mathrm{c}$ is rewritten as

$$\begin{aligned}
&\mathbb{P}\left(\mathtt{SINR}_\ell(y) \geq T\right) \\
&\quad = \mathbb{P}\left(\|\mathbf{H}_o\|_F^2 \geq \frac{S_\ell T}{P_\ell y^{-\alpha_\ell}} \left(\sum_{k=1}^{K} \sum_{\mathsf{x}_i \in \Phi_k^o} \mathsf{I}_{i,\mathrm{eqv}} + \sigma^2\right)\right) \\
&\quad \overset{\text{(a)}}{=} \sum_{m=0}^{NM_\ell - 1} \frac{(-1)^m}{m!} \mathbb{E}_{\mathsf{Y}}\left[(-1)^m \mathsf{Y}^m e^{-\mathsf{Y}}\right] \\
&\quad \overset{\text{(b)}}{=} \sum_{m=0}^{NM_\ell - 1} \frac{(-1)^m}{m!} \frac{\mathrm{d}^m}{\mathrm{d}s^m} \Big[\mathcal{L}_{\mathsf{Y}}(s)\Big]_{s=1},
\end{aligned} \quad (24)$$

where in (a) we define $\mathsf{Y} \triangleq \frac{S_\ell T}{P_\ell y^{-\alpha_\ell}} (\sum_{k=1}^{K} \sum_{\mathsf{x}_i \in \Phi_k^o} \mathsf{I}_{i,\mathrm{eqv}} + \sigma^2)$ and (b) follows from the differentiation rule for Laplace transforms. With Lemma 3, $\mathcal{L}_{\mathsf{Y}}(s)$ can be obtained as

$$\begin{aligned}
\mathcal{L}_{\mathsf{Y}}(s) = \exp\Bigg(&- \frac{s S_\ell T}{\mathtt{SNR}_\ell(y)} - \pi \sum_{k=1}^{K} \lambda_k \hat{P}_k^{2/\alpha_k} y^{2/\hat{\alpha}_k} \\
&\times \left[{}_2F_1\Big(-\tfrac{2}{\alpha_k}, S_k, 1 - \tfrac{2}{\alpha_k}; -\tfrac{sT}{\hat{S}_k}\Big) - 1\right]\Bigg),
\end{aligned} \quad (25)$$

where $\mathtt{SNR}_\ell(y) \triangleq P_\ell y^{-\alpha_\ell}/\sigma^2$ is the average signal-to-noise ratio and $\hat{S}_k \triangleq S_k/S_\ell$. De-conditioning on y and ℓ yields the final result. ∎

B. Proof of Theorem 2

Applying the law of total probability and making use of Lemma 1 and (19), we can rewrite (7) as

$$\mathtt{P_c} = \sum_{\ell=1}^{K} A_\ell \int_0^\infty f_{\mathtt{y},\ell}(y)\, \mathbb{P}\left(\mathtt{SINR}_\ell(y) \geq T\right) \mathrm{d}y. \quad (26)$$

Next, we focus on $\mathbb{P}\left(\mathtt{SINR}_\ell(y) \geq T\right)$, which after conditioning on Φ^o, yields

$$\begin{aligned}&\mathbb{E}_{\Phi^o}\left[\mathbb{P}(\mathtt{SINR}_{1,\ell}(y) \geq T - \mathtt{SINR}_{2,\ell}(y)|\Phi^o)\right]\\ &= \mathbb{E}_{\Phi^o}\left[\int_0^\infty \mathbb{P}(\mathtt{SINR}_{1,\ell}(y) \geq T - z|\Phi^o)\, f_{\mathtt{SINR}_{2,\ell}(y)|\Phi^o}(z)\, \mathrm{d}z\right],\end{aligned} \quad (27)$$

where we have defined

$$\mathtt{SINR}_{n,\ell}(y) \triangleq \frac{P_\ell}{M_\ell y^{\alpha_\ell}} \frac{\|\mathbf{h}_{o,n}\|_F^2}{\mathsf{I}_n + \sigma^2}. \quad (28)$$

Applying the same steps as in (24), the first term inside the integral in (27) can be evaluated as

$$\begin{aligned}&\mathbb{P}(\mathtt{SINR}_{1,\ell}(y) \geq T - z|\Phi^o)\\ &= \sum_{m=0}^{M_\ell - 1} \frac{(-1)^m}{m!} \frac{\mathrm{d}^m}{\mathrm{d}s^m}\left[\exp\left(-\frac{sM_\ell(T-z)^+}{\mathtt{SNR}_\ell(y)}\right)\right.\\ &\left.\times \prod_{k=1}^{K}\prod_{\mathsf{x}_i \in \Phi_k^o}\left(1 + \frac{s\,(T-z)^+ \hat{P}_k y^{\alpha_\ell}}{\hat{M}_k \|x_i\|^{\alpha_k}}\right)^{-M_k}\right]_{s=1}.\end{aligned} \quad (29)$$

Similarly, we have

$$\begin{aligned}f_{\mathtt{SINR}_2|\Phi^o}(z) &= \frac{\mathrm{d}}{\mathrm{d}w}\Big[\mathbb{P}\left(\mathtt{SINR}_2 \leq w\right)\Big]_{w=z}\\ &= \frac{(-1)^{M_\ell}}{z\,\Gamma(M_\ell)} \frac{\mathrm{d}^{M_\ell}}{\mathrm{d}t^{M_\ell}}\left[\exp\left(-\frac{tM_\ell z}{\mathtt{SNR}_\ell(y)}\right)\right.\\ &\left.\times \prod_{k=1}^{K}\prod_{\mathsf{x}_i \in \Phi_k^o}\left(1 + \frac{tz\hat{P}_k y^{\alpha_\ell}}{\hat{M}_k \|x_i\|^{\alpha_k}}\right)^{-M_k}\right]_{t=1}.\end{aligned} \quad (30)$$

By Fubini's Theorem, the expectation $\mathbb{E}_{\Phi^o}[\cdot]$ can be moved inside the integral over z in (27). By Leibniz integration rule for infinite integrals [22], the differentiations $\mathrm{d}^m/\mathrm{d}s^m$ in (29) and $\mathrm{d}^{M_\ell}/\mathrm{d}t^{M_\ell}$ in (30) can be moved outside $\mathbb{E}_{\Phi^o}$. Since the Φ_k^o are independent, we then have

$$\begin{aligned}&\mathbb{E}\left[\prod_{k=1}^{K}\prod_{\mathsf{x}_i \in \Phi_k^o}\left(1 + \frac{s\,(T-z)^+ \hat{P}_k y^{\alpha_\ell}}{\hat{M}_k \|\mathsf{x}_i\|^{\alpha_k}}\right)^{-M_k}\left(1 + \frac{tz\hat{P}_k y^{\alpha_\ell}}{\hat{M}_k \|\mathsf{x}_i\|^{\alpha_k}}\right)^{-M_k}\right]\\ &= \exp\left\{-\pi \sum_{k=1}^{K} \lambda_k \hat{P}_k^{2/\alpha_k} y^{2/\hat{\alpha}_k}\, \Psi\left(\tfrac{s}{\hat{M}_k}(T-z)^+, \tfrac{tz}{\hat{M}_k}, M_k, \alpha_k\right)\right\},\end{aligned} \quad (31)$$

where $\hat{M}_k \triangleq M_k/M_\ell$ and

$$\Psi(a_1, a_2, p, q) = \int_1^\infty 1 - \left[\left(1 + \frac{a_1}{u^{q/2}}\right)\left(1 + \frac{a_2}{u^{q/2}}\right)\right]^{-p} \mathrm{d}u. \quad (32)$$

Combining (26) – (31) yields the result. ∎

REFERENCES

[1] J. G. Andrews *et al.*, "What will 5G be?" *IEEE J. Sel. Areas Commun.*, vol. 32, no. 6, pp. 1065–1082, Jun. 2014.

[2] 3GPP, "Further advancements for E-UTRA," TR 36.213, Tech. Rep., Mar. 2008.

[3] D. G. Brennan, "Linear diversity combining techniques," *Proc. IEEE*, vol. 91, no. 2, pp. 331–356, Feb. 2003.

[4] X. Cui, Q. Zhang, and Z. Feng, "Outage performance for maximal ratio combiner in the presence of unequal-power co-channel interferers," *IEEE Commun. Lett.*, vol. 8, no. 5, pp. 289–291, May 2004.

[5] A. M. Hunter, J. G. Andrews, and S. Weber, "Transmission capacity of ad hoc networks with spatial diversity," *IEEE Trans. Wireless Commun.*, vol. 7, no. 12, pp. 5058–5071, Dec. 2008.

[6] A. Chopra and B. L. Evans, "Joint statistics of radio frequency interference in multiantenna receivers," *IEEE Trans. Signal Process.*, vol. 60, no. 7, pp. 3588–3603, Jul. 2012.

[7] R. Tanbourgi, H. S. Dhillon, J. G. Andrews, and F. K. Jondral, "Effect of spatial interference correlation on the performance of maximum ratio combining," *IEEE Trans. Wireless Commun.*, vol. 13, no. 6, pp. 3307–3316, June 2014.

[8] ——, "Dual-branch MRC receivers under spatial interference correlation and Nakagami fading," *IEEE Trans. Commun.*, vol. 62, no. 6, pp. 1830–1844, Jun. 2014.

[9] ——, "Dual-branch MRC receivers in the cellular downlink under spatial interference correlation," in *European Wireless Conference*, May 2014.

[10] A. Ghosh *et al.*, "Heterogeneous cellular networks: From theory to practice," *IEEE Commun. Mag.*, vol. 50, no. 6, pp. 54–64, Jun. 2012.

[11] J. G. Andrews, F. Baccelli, and R. K. Ganti, "A tractable approach to coverage and rate in cellular networks," *IEEE Trans. Commun.*, vol. 59, no. 11, pp. 3122 –3134, Nov. 2011.

[12] H. S. Dhillon, R. K. Ganti, F. Baccelli, and J. G. Andrews, "Modeling and analysis of *K*-tier downlink heterogeneous cellular networks," *IEEE J. Sel. Areas Commun.*, vol. 30, no. 3, pp. 550–560, Apr. 2012.

[13] D. Stoyan, W. Kendall, and J. Mecke, *Stochastic Geometry and its Applications*, 2nd ed. Wiley, 1995.

[14] S. Singh, H. S. Dhillon, and J. G. Andrews, "Offloading in heterogeneous networks: Modeling, analysis, and design insights," *IEEE Trans. Wireless Commun.*, vol. 12, no. 5, pp. 2484–2497, Dec. 2013.

[15] A. Shah and A. Haimovich, "Performance analysis of maximal ratio combining and comparison with optimum combining for mobile radio communications with cochannel interference," *IEEE Trans. Veh. Technol.*, vol. 49, no. 4, pp. 1454–1463, Jul 2000.

[16] E. G. Larsson and P. Stoica, *Space-Time Block Coding for Wireless Communications*, 1st ed. Cambridge University Press, 2008.

[17] T. Benedict and T. Soong, "The joint estimation of signal and noise from the sum envelope," *IEEE Trans. Inf. Theory*, vol. 13, no. 3, pp. 447–454, Jul. 1967.

[18] D. Pauluzzi and N. Beaulieu, "A comparison of SNR estimation techniques for the AWGN channel," *IEEE Trans. Commun.*, vol. 48, no. 10, pp. 1681–1691, Oct. 2000.

[19] A. Paulraj, R. Nabar, and D. Gore, *Introduction to Space-Time Wireless Communications*, 1st ed. Cambridge University Press, 2003.

[20] V. Tarokh, H. Jafarkhani, and A. Calderbank, "Space-time block codes from orthogonal designs," *IEEE Trans. Inf. Theory*, vol. 45, no. 5, pp. 1456–1467, Jul. 1999.

[21] Y. Shang, "Space-time code designs and fast decoding for MIMO and cooperative communication systems," Ph.D. dissertation, University of Delaware, 2008.

[22] F. W. Olver *et al.*, *NIST Handbook of Mathematical Functions*, 1st ed. Cambridge University Press, 2010.

[23] A. Goldsmith, *Wireless Communications*. Cambridge University Press, 2005.

[24] 3GPP, "Further advancements for E-UTRA," TR 36.814, Tech. Rep., Mar. 2009.

[25] H.-S. Jo, Y. J. Sang, P. Xia, and J. G. Andrews, "Heterogeneous cellular networks with flexible cell association: A comprehensive downlink SINR analysis," *IEEE Trans. Wireless Commun.*, vol. 11, no. 10, pp. 3484–3495, Oct. 2012.

[26] W. Feller, *An Introduction to Probability Theory and Its Applications, Vol. 2*, 2nd ed. Wiley, Jan. 1971.

[27] R. Tanbourgi and F. K. Jondral, "Analysis of heterogeneous cellular networks under frequency diversity and interference correlation," *IEEE Wireless Commun. Lett.*, vol. 4, no. 1, pp. 2–5, Feb 2015.